Heterogeneous integration of monolithic LED-PD with circuitry for intensity-stabilization

X. Ma, H. Lyu, Y. F. Cheung and H.W. Choi, *Senior Member, IEEE*

***Abstract*—The monolithic integration of a photodiode (PD) to a light-emitting diode (LED) enables the on-chip monitoring of light output intensity from the emitter. The light output intensity from the LED, which would fluctuate and degrade over time, can be stabilized with the aid of a driver circuit that reads the photocurrent from the on-chip PD as a feedback signal. Previous demonstration of such systems, implemented with feedback driver circuits built with microcontroller boards or analog circuit assembled on printed circuit boards (PCBs), showed that the intensity can be stabilized to within 0.03%, albeit with dimensions disproportionate to the LED-PD chip itself. A simplified circuit consisting of a transimpedance amplifier (TIA), proportional-integral (PI) controller and a low-dropout (LDO) regulator is heterogeneously ~~integration~~ integrated with the LED-PD as a system-in-package (SiP), making use of bare dies for the majority of components. Using this approach, the entire system is shrunk to a dimension of 4 mm × 5 mm, which is comparable to the size of the LED-PD chip. The reduced footprint facilitate practical applications of the LED-PD devices for intensity-stabilized lighting or displays. The stability is further improved to 0.01% on average over one-hour periods based on the on-chip PD photocurrent, while the power efficiency is improved to over 70%.**

***Index Terms*—Light-emitting diodes, Photodiodes, Heterogeneously integrated circuits.**

I. Introduction

GAN based light-emitting diodes (LEDs) have many distinct advantages over their predecessors, including energy conversion efficiencies, longevity, compactness and robustness. Nevertheless, LEDs require drivers that provide constant voltage output or constant current output for operation. Typically, the LEDs and the driver integrated circuit (IC) dies are individually packaged which are then soldered onto a printed circuit board (PCB) and electrically connected through interconnects in a luminaire. As a result, the efficiency of the luminaire is inevitably reduced, comprising the compactness and robustness of the system at the same time. To overcome this shortcoming, tighter integration of the components and modules is desirable.

Monolithic integration, whereby multiple devices and components are integrated at a chip-scale level, offers the highest degree of functionality, performance, compactness and robustness, as evident from the Si ICs. Given that different types of devices have been developed from the GaN material system including optoelectronic devices such as LEDs and laser diodes [1] and electronic devices such as transistors [2], [3], monolithic integration of GaN devices is feasible. The monolithic integration of LEDs, PDs and waveguides have been reported in [4]–[7]. There are also numerous reports on the integration of LEDs and high-electron-mobility transistors (HEMTs) on a wafer level [8]–[11]. However, the very different structures between the LEDs with InGaN/GaN multi-quantum wells (MQWs) and the HEMTs with AlGaN/GaN two-dimensional electron gas (2DEG) means that such integration tasks ~~remain challenging~~ are challenging as complicated epitaxial design and growth are involved, implying additional production costs. Through selective-area epitaxy growth, GaN LEDs and electronic devices have successfully been integrated monotonically in [12]–[15] . Moreover, the monolithic integration of MOSFETs, transmitters, waveguides, and receivers without re-growth or post-growth doping is reported in [16]. However, when the functionality of the system becomes increasingly complex, requiring devices beyond LEDs and transistors, the tasks will be even more challenging.

On the other hand, heterogeneous integration provides a practical alternative. [17], [18] It may not offer the level of tightness that monolithic integration provides, but it allows the use of optimized chips built on optimal materials. For instance, the heterogeneous integration of GaN LEDs and Si ICs combines the merits of the respective materials to build functional systems not otherwise achievable based on a system-in-package (SiP) approach [19]. Additionally, cost-savings can be expected as bare dies cost less than packaged ICs. In this work, a heterogeneously integrated system comprising a monolithically-integrated GaN-based LED-PD and Si-based LED driver with feedback circuitry is demonstrated. Being fabricated on the same wafer, the PD with dimensions of 100 × 400 μm^2 has identical device structure as the adjacent 1000 × 1000 μm^2 LED. The integrated system enables the LED to emit intensity-stabilized light output in a compact footprint.

The light output from an LED is known to fluctuate randomly [20], [21] and degrade non-linearly over time [22]–[24]. The monolithically-integrated LED-PD device was proposed to provide an intensity-stabilized solution. Apart from light emission through recombination, the MQWs in an LED structure are capable of light detection through optical absorption. In view of this property, an additional LED that operates and functions as a PD can be monolithically integrated with the emitter LED for light detection. Details on the mechanism, fabrication and operation of the device can be found in ref. [4], [5], [25]. Variations in the light output of the LED will trigger a proportional variation to the photocurrent of the on-chip PD. By monitoring the photocurrent, the LED driving voltage or current can be adjusted to provide a constant

X. Ma, H. Lyu, Y.F. Cheung and H.W. Choi are with the Department of Electrical and Electronic Engineering, The University of Hong Kong, Hong Kong SAR

Manuscript received xxxxxx; revised xxxxxx

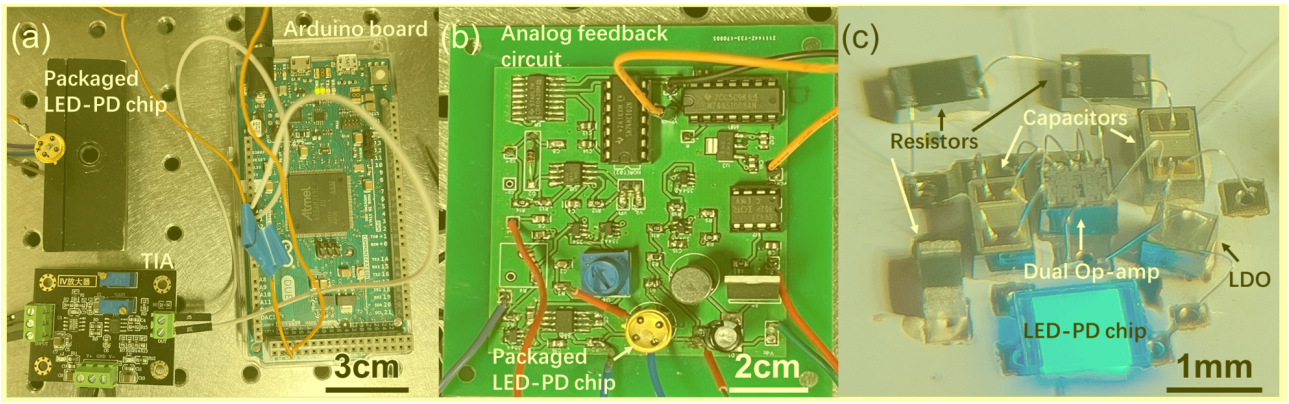

Fig. 1. Images of the intensity-stabilized LED systems using (a) microcontroller based digital control circuit; (b) analog control circuit assembled on PCB and (c) heterogeneously integrated system-in-package.

intensity output [26], a task that requires additional circuitry. As reported in [4], [5], the photocurrent is firstly amplified by a transimpedance amplifier (TIA) so that the photovoltage signal can be processed by either a microcontroller board (Arduino) or an analog circuit. These feedback-cum-driver circuits are very bulky compared with the LED-PD chips themselves, diminishing the compactness brought about by monolithic integration of the LED and PD, making it impractical to be applied in applications that call for high densities of LEDs such as arrays. A heterogeneous approach is adopted whereby the individual components in various formats including bare dies and SMDs are assembled as a SiP by a combination of wire-bonding and flip-chip bonding. By mainly using bare dies instead of individually packaged components to assemble the re-designed circuit, the entire system is shrunk to a footprint of 4 mm by 5 mm which is on par with the dimensions of a typical packaged LED, enhancing the practicality of the intensity-stabilized LED-PD concept. The design, assembly, characterization and performance of this integrated system will be reported in this paper, with emphasis on the intensity stabilization performance in the shorter-term (of up to 10 hours).

II. CIRCUIT DESIGN

The external feedback circuit reported in [4] was built based on an Arduino microcontroller board, providing digital feedback and driving voltage to achieved stabilized light output. While the circuit significantly reduced the fluctuation and degradation of the LED light output intensity compared with a driver circuit without feedback from a variance of 1% on average over one-hour periods to 0.13% and 0.43% according to on-chip PD and external photosensor, respectively, the precision of the feedback signal was restricted by the bit depth of the digital system. The bulkiness of the system as illustrated in Fig. 1(a), and the high power consumption of 2.27 W (power efficiency of 2.77%) at LED injection current of 20 mA also limited its practicality. As such, an analog feedback circuit was designed to replace the Arduino board [5], with further improvement in stability to a variance of 0.03% according to the on-chip PD. The circuit, consisting of over 40 individual components including op-amps, flip-flops, and power MOSFETs, are assembled on a PCB of 8.2 cm × 8.2 cm as shown in Fig. 1(b), which is still much larger than the 1.2 mm × 1 mm LED-PD chip, although power consumption was reduced to 205 mW (power efficiency of 29%) when the injection current of the LED is 20 mA.

To overcome the above-mentioned issues, a new analog feedback circuit is designed as shown in Fig. 2, employing a low-dropout (LDO) regulator for driving the LED with the target of minimizing footprint. The photocurrent generated by the on-chip PD is converted to a photovoltage by the TIA $V_{TIA,out}$. The photovoltage signal is read by the proportional-integral (PI) controller, whose output voltage $V_{PI,out}$ will be adjusted according to the difference between the photovoltage and the reference voltage V_{Ref} which determines the nominal stabilized light output intensity of the LED.

Since $V_{PI,out}$ is connected to the GND pin of the LDO, its output voltage $V_{LDO,out}$ is given by $V_{PI,out}$ + 3 V when a 3 V LDO (TPS71530) is used. In other words, the circuit provides a variable $V_{LDO,out}$ to drive the LED with a target of maintaining $V_{TIA,out}$ at V_{Ref}. For instance, when the light output intensity of the LED drops due to fluctuation or degradation, the photocurrent and the amplified photovoltage $V_{TIA,out}$ drops correspondingly to below the setpoint, triggering an increase of $V_{PI,out}$ until the $V_{TIA,out} = V_{Ref}$, so that the LED light output intensity is restored to the stabilized level.

The transfer function of a PI controller is given by:

$$G(s) = k_p + \frac{k_i}{s} = k_p + \frac{k_p}{T} \times \frac{1}{s}$$

where k_p is the proportional gain, k_i is the integral gain, and T is the time constant. In this project, k_p is tuned to be 1 so that the time constant T and k_i are calculated to be ~100 µs and 10^4, respectively. These parameters provide response that strikes a good balance between speed and stability, offering a low level of error in the steady state. In the implementation of the analog PI controller circuit, k_p=R_2/R_1 and k_i=$1/R_1C_1$. With R_1 chosen to be 1 kΩ, the values of R_2 and C_1 are determined to be 1 kΩ and 100 nF, respectively.

The functionality of the circuit is verified through PSPICE simulations, with the LED-PD device modeled as a diode (turn on voltage=2.3 V, forward resistance=25 Ω) and a Current Control Current Source (CCCS) as the photocurrent of the

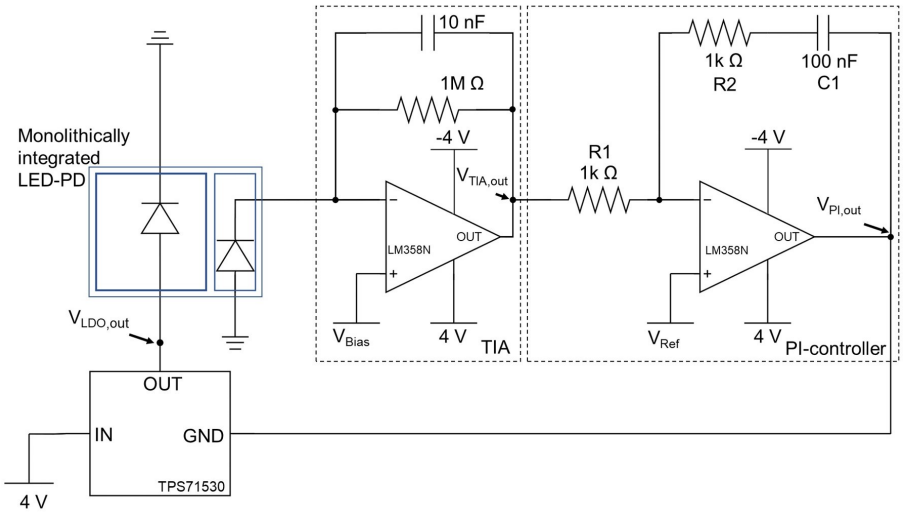

Fig. 2. Circuit diagram of the light intensity stabilization feedback control system.

PD depends on the light output from the LED, which in turn depends on the injection current. The gain of the CCCS is 7×10^{-5} as determined from experimental measurements.

An additional current source is connected in parallel to the PD for applying a small fluctuating current to simulate the fluctuating output light intensity of the LED. Fig. 3 shows the plots of $V_{TIA,out}$ and $V_{LDO,out}$ in response to the randomly fluctuating current. As can be seen, $V_{TIA,out}$ is maintained to the value of V_{Ref} by adjustment of $V_{LDO,out}$.

III. RESULTS AND DISCUSSION

The verified circuit is assembled as a heterogeneously system on a custom-designed fiberglass PCB substrate with the in-house fabricated monolithic LED-PD chip and commercially-sourced components. All the ICs and passive components are in wire-bondable bare die formats, except for the 1MΩ resistor which is a 0402 SMD package. The LED-PD chip is mounted in a flip-chip configuration, while the remaining chips are mounted with die-bond epoxy and wire-bonded. The entire circuit occupies a space of 4 mm × 5 mm on the substrate, as shown in Fig. 1(c).

As the random fluctuation and degradation of the LED cannot be controlled manually, a randomly fluctuating V_{Ref} signal generated by an arbitrary wave generator (AWG, Siglent SDG6022X) is applied instead to emulate those fluctuations. A change of V_{Ref} will temporarily induce a difference between $V_{TIA,out}$ and V_{Ref} so that the feedback circuit will immediately adjust $V_{LDO,out}$ to equalize $V_{TIA,out}$ to V_{Ref}. This produces the same effect as fluctuations of LED light intensity. Therefore, the fluctuating V_{Ref} can be considered as an inverted signal of the random fluctuations to the feedback circuit. Fig. 4 shows the plots of $V_{TIA,out}$ and $V_{LDO,out}$ in response to the randomly fluctuating V_{Ref}. As can be seen, $V_{TIA,out}$ is capable of tracking V_{Ref} by adjustment of $V_{LDO,out}$. The performance of the heterogeneously integrated system is tested using the setup shown in Fig. 5. The entire system is powered by a benchtop power supply (Keithley 2230G-30-1) while the light output intensity of the LED is monitored $V_{TIA,out}$ with an oscilloscope

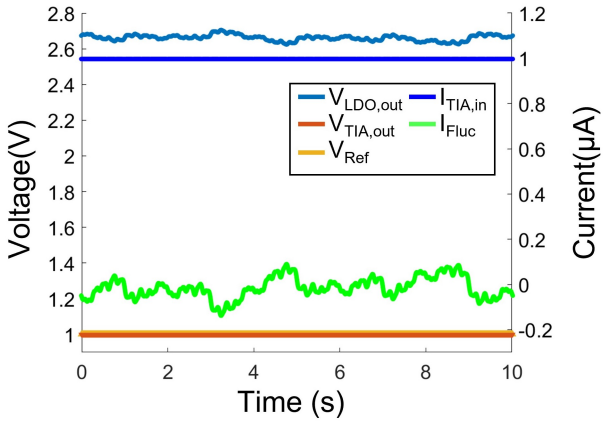

Fig. 3. Simulated $V_{LDO,out}$ and $V_{TIA,out}$ when a fluctuating current (I_{Fluc}) is applied across the CCCS.

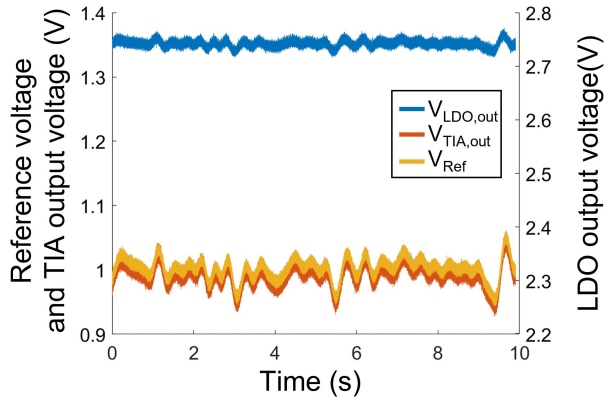

Fig. 4. Measured $V_{LDO,out}$ and $V_{TIA,out}$ when a fluctuating $V_{LDO,out}$ and V_{Ref} is applied.The bias current of the LED is ~14 mA

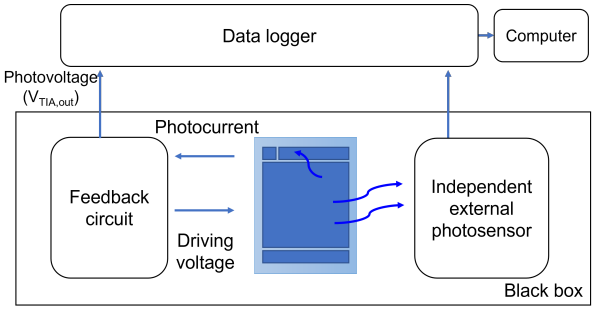

Fig. 5. Experimental setup for testing of the system.

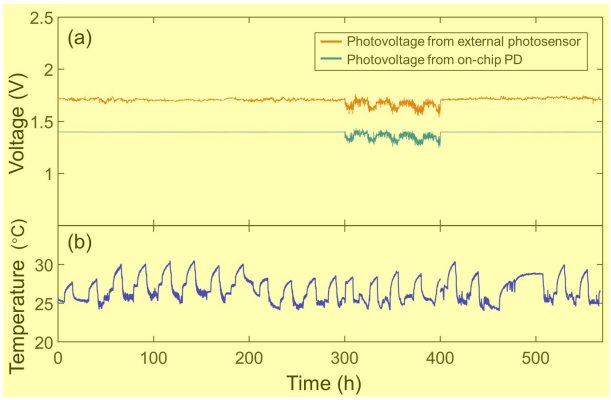

Fig. 6. (a) Measured photovoltages from the on-chip PD and the external photosensor. (b) Ambient temperature during the testing period.

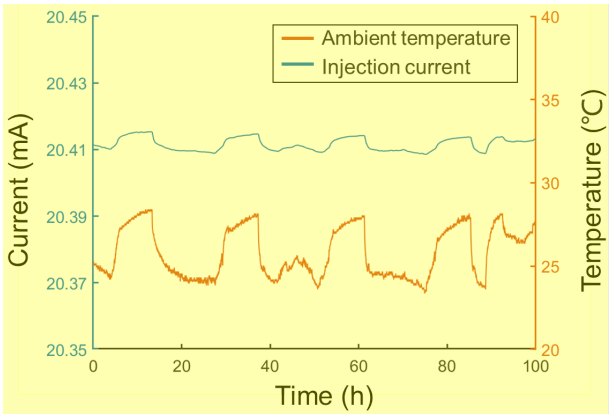

Fig. 7. The injection current of an LED driven by a constant voltage at room temperature, averaged over 20-minute periods.

(Agilent DSO9404A). To verify the functionality and accuracy of the on-chip PD, the signal from an external photosensor (AMS TSL-250R-LF) mounted ~2 cm away from the LED is used as an independent reference monitor. Both photovoltages from the on-chip PD and the external photosensor are simultaneously recorded by a data logger (Picolog ADC-24). The entire testing platform is placed within a dark enclosure to eliminate the influence of ambient lighting to the readings. Due to limited hours of air-conditioning provided in the testing environment, the temperature is not maintained. Nevertheless, the non-temperature-stabilized serves to test the ability of the system to maintain a stable light output despite fluctuating temperatures.

The recorded data is plotted in the Fig. 6. The photovoltages are recorded for a total of 570 hours at a logging interval of 10 seconds as plotted in Fig. 6(a). For reference, the temperature of the environment is logged and plotted in Fig. 6(b). Intensity regulation is tested during the first 300 hours of testing, with V_{ref} is set to 1.4 V. The variation of the photovoltage is 0.3% and 0.01% on average over one-hour periods, according to the recorded photovoltages of the external photosensor and the on-chip PD, respectively, while the variation over 10-hour periods is slightly increased to 0.4% and 0.02% on average in spite of temperature variations of 5°C on a daily basis. Within this period, the output voltage of the LDO $V_{LDO,out}$ has varied by over 100 mV in order to regulate the light output intensity of the LED. The feedback circuit is turned off in the next 100 hours of testing so that LED is directly driven by a constant voltage of 2.85 V from the LDO. The variations of photovoltages from both detectors increased to 1.2% on average over 1-hour periods which is consistent with the reported data in [4] and 2.5% on average over 10-hour periods. Note that the variations in photovoltages are largely in sync with the variations in temperatures, with periods of elevated temperatures correlated to periods of reduced photovoltages. Such variations may be caused by (1) variations in light output, (2) variations in photocurrent or (3) variations in driving current. The temperature sensitivity of the PD has been investigated in [4] by monitoring the photocurrent under constant illumination across the temperature range of 25 to 100 °C, from which a temperature coefficient of 0.02 %/°C is determined. To study the effects of temperature on the driving current provided by the LDO, variations in injection current and temperature over 100 hours is recorded and plotted in Fig. 7, from which a 0.005 %/°C dependence is evaluated. In comparison, the dependence of photovoltage with temperature is evaluated as ~0.8 %/°C. Therefore, fluctuations in light output is mainly responsible for the observed fluctuations in photovoltages, since radiative recombination efficiency reduces with increasing temperature in this temperature range [27], [28]. After a period of operation without feedback, the feedback system is turned on again for a further 170 hours of testing, during which photovoltage variations are restored to 0.28% and 0.01% over one-hour periods and 0.37% and 0.02% over 10-hour periods for the external photosensor and on-chip PD, respectively. The data shows that the circuit, despite being simplified, is fully functional with regulation performance on par with or better than previous circuit designs, not to mention the significant reductions in footprints.

At steady state, $V_{LDO,out}$ is measured to be 2.85 V when V_{Ref}=1.4 V (photocurrent =1.4 μA), which is also the input voltage to the LED. At this voltage, $I_{LED,in}$ = 19.9 mA as evaluated from the IV curve. The power supply delivers a current of 20.2 mA at a voltage of 4 V, thus with power consumption of 80.8 mW. The power efficiency of the system is determined to be 70.2% by taking the ratio between the power consumption of the LED to the power supply. Compared to the circuit reported in [5] whose power efficiency is <30%, this simplified circuit provides more than twice the power efficiency.

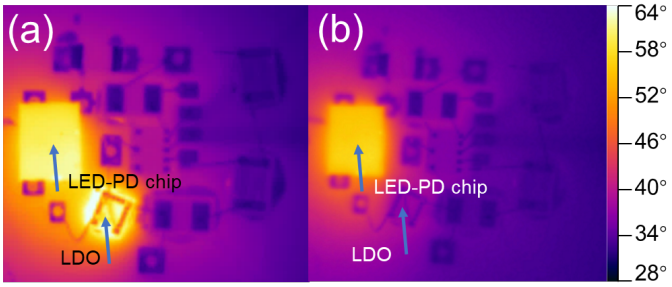

Fig. 8. LWIR image of the heterogeneously integrated SiP when (a) LED is driven by the integrated LDO and (b) LED is driven by an external LDO.

As the components are assembled at a much tighter density compared to previous implementations, thermal analysis on the integrated system is investigated by longwave-infrared (LWIR) thermometry. An LWIR image of the operating device is captured by a FLIR camera (SC645) when V_{Ref} =1.4 V as shown in Fig. 8(a). At this operating point, the power consumption of the LED and the LDO are 56.72 mW and ~~24.08 mW~~22.88 mW, respectively, which are the main heat sources amongst all components in the system. According to the LWIR image, both chips sustain surface temperatures of up to 63.8°C, although the LED corner closer to the LDO is mildly hotter than the farther corner by 2.8°C. When the LED is driven by an external but identical LDO source, the temperature at the center of the LED dropped from 61°C to 57.5°C, as shown in Fig. 8(b). The results illustrate that the tight integration of chips, especially the active devices, does introduce mild thermal loading effects, which can be mitigated by careful design of chip layout, and the use of a substrate with higher thermal conductivity, such as copper.

IV. CONCLUSION

In summary, an intensity-stabilized LED based on heterogeneous integration of a monolithically integrated GaN LED-PD chip and a control circuit assembled mainly with bare die components is demonstrated in this work. This system is able to maintain the stability of the light output intensity of the LED to variations of ~0.01% on average over one-hour periods, with power efficiencies of over 70% when the injection current of the LED is ~20 mA. These figures represent significant improvements over previous systems assembled with external control circuits, which occupy dimensions much larger than this 4mm × 5mm system-in-package, as well as cost-savings associated with the use of bare dies and simplified assembly processes.

REFERENCES

[1] M. C. Schmidt, K.-C. Kim, R. M. Farrell, D. F. Feezell, D. A. Cohen, M. Saito, K. Fujito, J. S. Speck, S. P. DenBaars, and S. Nakamura, "Demonstration of nonpolar m-plane ingan/gan laser diodes," *Japanese journal of applied physics*, vol. 46, no. 3L, p. L190, 2007.

[2] K. Joshin, T. Kikkawa, S. Masuda, and K. Watanabe, "Outlook for gan hemt technology," *Fujitsu Sci. Tech. J*, vol. 50, no. 1, pp. 138–143, 2014.

[3] J. W. Chung, W. E. Hoke, E. M. Chumbes, and T. Palacios, "Algan/gan hemt with 300-ghz $f_{\max}$," *IEEE Electron Device Letters*, vol. 31, no. 3, pp. 195–197, 2010.

[4] K. H. Li, H. Lu, W. Y. Fu, Y. F. Cheung, and H. W. Choi, "Intensity-stabilized leds with monolithically integrated photodetectors," *IEEE Transactions on Industrial Electronics*, vol. 66, no. 9, pp. 7426–7432, 2018, doi: 10.1109/TIE.2018.2873522.

[5] K. H. Li, Y. F. Cheung, W. Jin, W. Y. Fu, A. T. L. Lee, S. C. Tan, S. Y. Hui, and H. W. Choi, "Ingan rgb light-emitting diodes with monolithically integrated photodetectors for stabilizing color chromaticity," *IEEE Transactions on Industrial Electronics*, vol. 67, no. 6, pp. 5154–5160, 2020, doi: 10.1109/TIE.2019.2926038.

[6] J. Li, J. Wu, L. Chen, X. An, J. Yin, Y. Wu, L. Zhu, H. Yi, and K. H. Li, "On-chip integration of iii-nitride flip-chip light-emitting diodes with photodetectors," *Journal of Lightwave Technology*, vol. 39, no. 8, pp. 2603–2608, 2021.

[7] K. H. Li, W. Y. Fu, Y. F. Cheung, K. K. Y. Wong, Y. Wang, K. M. Lau, and H. W. Choi, "Monolithically integrated ingan/gan light-emitting diodes, photodetectors, and waveguides on si substrate," *Optica*, vol. 5, no. 5, pp. 564–569, May 2018. [Online]. Available: https://opg.optica.org/optica/abstract.cfm?URI=optica-5-5-564

[8] C. Liu, Y. Cai, X. Zou, and K. M. Lau, "Low-leakage high-breakdown laterally integrated hemt-led via n-gan electrode," *IEEE Photonics Technology Letters*, vol. 28, no. 10, pp. 1130–1133, 2016.

[9] K. H. Li, W. Y. Fu, and H. W. Choi, "Chip-scale gan integration," *Progress in Quantum Electronics*, vol. 70, p. 100247, 2020. [Online]. Available: https://www.sciencedirect.com/science/article/pii/S007967272030001X

[10] Z. J. Liu, T. Huang, J. Ma, C. Liu, and K. M. Lau, "Monolithic integration of algan/gan hemt on led by mocvd," *IEEE Electron Device Letters*, vol. 35, no. 3, pp. 330–332, 2014.

[11] Y. Cai, X. Zou, C. Liu, and K. M. Lau, "Voltage-controlled gan hemt-led devices as fast-switching and dimmable light emitters," *IEEE Electron Device Letters*, vol. 39, no. 2, pp. 224–227, 2018.

[12] Z. Li, J. Waldron, T. Detchprohm, C. Wetzel, R. Karlicek Jr, and T. Chow, "Monolithic integration of light-emitting diodes and power metal-oxide-semiconductor channel high-electron-mobility transistors for light-emitting power integrated circuits in gan on sapphire substrate," *Applied Physics Letters*, vol. 102, no. 19, p. 192107, 2013.

[13] Y.-J. Lee, Z.-P. Yang, P.-G. Chen, Y.-A. Hsieh, Y.-C. Yao, M.-H. Liao, M.-H. Lee, M.-T. Wang, and J.-M. Hwang, "Monolithic integration of gan-based light-emitting diodes and metal-oxide-semiconductor field-effect transistors," *Optics Express*, vol. 22, no. 106, pp. A1589–A1595, 2014.

[14] C. Liu, Y. Cai, Z. Liu, J. Ma, and K. M. Lau, "Metal-interconnection-free integration of ingan/gan light emitting diodes with algan/gan high electron mobility transistors," *Applied Physics Letters*, vol. 106, no. 18, p. 181110, 2015.

[15] C. Liu, Y. Cai, H. Jiang, and K. M. Lau, "Monolithic integration of iii-nitride voltage-controlled light emitters with dual-wavelength photodiodes by selective-area epitaxy," *Optics Letters*, vol. 43, no. 14, pp. 3401–3404, 2018.

[16] J. Yan, L. Wang, B. Jia, Z. Ye, H. Zhu, H. Choi, and Y. Wang, "Uniting gan electronics and photonics on a single chip," *Journal of Lightwave Technology*, vol. 39, no. 19, pp. 6269–6275, 2021.

[17] W. Chen and B. Bottoms, "Heterogeneous integration roadmap: Driving force and enabling technology for systems of the future," in *2019 Symposium on VLSI Technology*. IEEE, 2019, pp. T50–T51.

[18] S. S. Iyer, "Heterogeneous integration for performance and scaling," *IEEE Transactions on Components, Packaging and Manufacturing Technology*, vol. 6, no. 7, pp. 973–982, 2016.

[19] F. Roozeboom, A. Kemmeren, J. Verhoeven, F. Van Den Heuvel, J. Klootwijk, H. Kretschman, T. Frič, E. Van Grunsven, S. Bardy, C. Bunel *et al.*, "Passive and heterogeneous integration towards a si-based system-in-package concept," *Thin Solid Films*, vol. 504, no. 1-2, pp. 391–396, 2006.

[20] J. Glemža, J. Matukas, S. Pralgauskaitė, and V. Palenskis, "Low-frequency noise characteristics of high-power white led during long-term aging experiment," *Lithuanian Journal of Physics*, vol. 58, no. 2, 2018.

[21] N. Bochkareva, A. Ivanov, A. Klochkov, and Y. Shreter, "Current noise and efficiency droop of light-emitting diodes in defect-assisted carrier tunneling from an ingan/gan quantum well," *Semiconductors*, vol. 53, no. 1, pp. 99–105, 2019.

[22] M. Meneghini, L.-R. Trevisanello, G. Meneghesso, and E. Zanoni, "A review on the reliability of gan-based leds," *IEEE Transactions on Device and Materials Reliability*, vol. 8, no. 2, pp. 323–331, 2008.

[23] G. Meneghesso, M. Meneghini, and E. Zanoni, "Recent results on the degradation of white leds for lighting," *Journal of Physics D: Applied Physics*, vol. 43, no. 35, p. 354007, 2010.

[24] M. Meneghini, A. Tazzoli, G. Mura, G. Meneghesso, and E. Zanoni, "A review on the physical mechanisms that limit the reliability of gan-based leds," *IEEE Transactions on Electron Devices*, vol. 57, no. 1, pp. 108–118, 2009.
[25] H. W. Choi, K. H. Li, and H. Lu, "Light-emitting diodes (LEDs) with monolithically-integrated photodetectors for in situ real-time intensity monitoring," May 23 2019, US Patent App. 16/300,329.
[26] F.-C. Wang, C.-W. Tang, and B.-J. Huang, "Multivariable robust control for a red–green–blue led lighting system," *IEEE transactions on Power Electronics*, vol. 25, no. 2, pp. 417–428, 2010.
[27] J. Liu, W. Tam, H. Wong, and V. Filip, "Temperature-dependent light-emitting characteristics of ingan/gan diodes," *Microelectronics Reliability*, vol. 49, no. 1, pp. 38–41, 2009. [Online]. Available: https://www.sciencedirect.com/science/article/pii/S0026271408003764
[28] C. Wang, J. Chen, C. Chiu, H.-C. Kuo, Y.-L. Li, T.-C. Lu, and S. Wang, "Temperature-dependent electroluminescence efficiency in blue ingan–gan light-emitting diodes with different well widths," *IEEE Photonics Technology Letters*, vol. 22, no. 4, pp. 236–238, 2010.

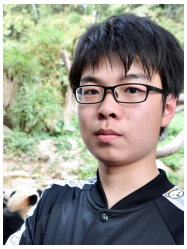

X. Ma is a PhD candidate at the University of Hong Kong, who is currently working on topics relating to GaN integration.

H. Lyu is a PhD candidate at the University of Hong Kong, who is currently working on topics relating to GaN micro-LEDs and integration.

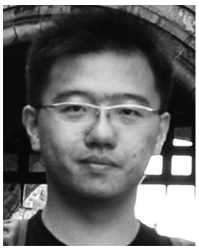

Y.F. Cheung received the M.Phil. degree in electrical and electronic engineering from the Department of Electrical and Electronic Engineering, The University of Hong Kong, Hong Kong, in 2013. He is currently a Research Engineer focusing on laser processing for devices, device characterizations and packaging. His current research projects are mainly specialized in different thin-film GaN devices, including vertical LEDs, flexible LEDs, etc.

H.W. Choi (SM'09) received the Ph.D. degree is electrical and electronics engineering from the National University of Singapore, Singapore, in 2003. He completed the postdoctoral training at the University of Strathclyde, Glasgow, U.K., where he contributed to pioneering development work on III-nitride emissive micro-light-emitting diode arrays. He is currently a Professor with the Department of Electrical and Electronic Engineering, the University of Hong Kong, Hong Kong. He currently leads a team of researchers investigating topics in GaN optoelectronics which include solid-state lighting, optical resonance and microcavities, integration, nanophotonics and laser processing of materials in the Semiconductor Lighting and Display Laboratory which he founded.